Faraday Discussions

Accepted Manuscript

This manuscript will be presented and discussed at a forthcoming Faraday Discussion meeting. All delegates can contribute to the discussion which will be included in the final volume.

Register now to attend! Full details of all upcoming meetings: http://rsc.li/fd-upcoming-meetings

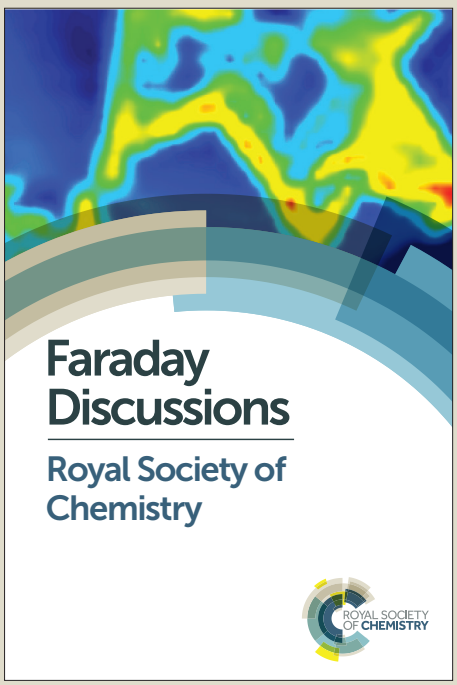

This is an *Accepted Manuscript*, which has been through the Royal Society of Chemistry peer review process and has been accepted for publication.

Accepted Manuscripts are published online shortly after acceptance, before technical editing, formatting and proof reading. Using this free service, authors can make their results available to the community, in citable form, before we publish the edited article. We will replace this *Accepted Manuscript* with the edited and formatted *Advance Article* as soon as it is available.

You can find more information about *Accepted Manuscripts* in the Information for Authors.

Please note that technical editing may introduce minor changes to the text and/or graphics, which may alter content. The journal's standard Terms & Conditions and the Ethical guidelines still apply. In no event shall the Royal Society of Chemistry be held responsible for any errors or omissions in this *Accepted Manuscript* or any consequences arising from the use of any information it contains.

ROYAL SOCIETY OF CHEMISTRY

www.rsc.org/faraday_d

Syngas Production by High Temperature Steam/CO_2 Coelectrolysis Using Solid Oxide Electrolysis Cells

Xinbing Chen, Chengzhi Guan, Guoping Xiao, Xianlong Du and Jian-Qiang Wang*

Shanghai Institute of Applied Physics, Chinese Academy of Sciences, Shanghai, China 201800

Abstract

High temperature (HT) steam/CO_2 coelectrolysis with solid oxide electrolysis cells (SOECs) using the electricity and heat generated from clean energies is an important alternative for syngas production without fossil fuel consumptions and greenhouse gas emissions. Herein, reaction characteristics and outlet syngas composition of HT steam/CO_2 coelectrolysis under different operating conditions, including distinct inlet gas compositions and electrolysis current densities, are systematically studied at 800°C using the commercially available SOECs. The HT coelectrolysis process, which has comparable performance to HT steam electrolysis, is more active than the HT CO_2 electrolysis process, indicating the important contribution of the reverse water-gas shift reaction in the formation of CO. The outlet syngas composition from HT steam/CO_2 coelectrolysis is very sensitive to the operation conditions, indicating the feasibility of controlling the syngas composition by varying the operating conditions. A maximum steam and CO_2 utilization of 77% and 76% is achieved at 1.0 A cm^{-2} with an inlet gas composition of 20% H_2 / 40 %

* Corresponding author. Tel: +86 21 3919 4051; fax: +86 21 3919 4051.
Email address: wangjianqiang@sinap.ac.cn.

steam/ 40% CO_2.

Keywords: Syngas production; High temperature steam/CO_2 coelectrolysis; Solid oxide electrolysis cells (SOECs); Reaction kinetics.

1. Introduction

Recently, HT steam/CO_2 coelectrolysis using SOECs, which electrochemically electrolyze CO_2 and steam into syngas ($CO+H_2$), provides an alternative to the traditional syngas production technologies including coal gasification and natural gas reforming, which release a lot of greenhouse gases and cause serious environmental concerns [1-4]. It is also highly valued as a crucial and limiting step in the CO_2 recycling process including CO_2 capture, dissociation and reuse due to its improved stability by reducing the possibility of carbon deposition associated with HT CO_2 electrolysis [5, 6]. When coupled with clean energies, such as solar, wind and nuclear energies, HT steam/CO_2 coelectrolysis can store the generated heat and power in the form of chemical energies in syngas that can be further processed into liquid fuels like synthetic diesel or dimethyl ether (DME) via catalytic reactions, thereby resolving the related energy storage issues as well as the supply-and-demand conflictions [7, 8]. Therefore, the development of HT coelectrolysis technologies bears great significance for the large-scale application of clean energies and reduction of CO_2 emissions.

Christopher Graves [9] et al. have made a review of different routes for steam/CO_2 dissociation, including thermolysis, thermochemical cycles,

electrolysis and photoelectrolysis, concluding that HT steam/CO_2 coelectrolysis with SOECs is the most efficient path with a potential electricity-to-syngas efficiency of ~100%. The process model established by Carl M. Stoots [10] at Idaho National Lab (INL) predicts an overall thermal-to-syngas efficiency of 48.3 ± 5.0% for large-scale HT steam/CO_2 coelectrolysis. Qingxi Fu [5] et al. have made an economic analysis of synthetic fuel production by using the syngas produced from HT steam/CO_2 coelectrolysis and the diesel production cost is estimated to be 0.86€/l, comparable to that of the biomass-to-liquid process. Therefore, HT steam/CO_2 coelectrolysis is a promising technology for syngas production with high efficiency and feasibility.

Compared with HT steam or CO_2 electrolysis, the study on HT steam/CO_2 coelectrolysis is much more complicated and the reasons include: (1) apart from electrochemical reactions (equation 1-2), the chemical reaction of reverse water-gas shift reaction (RWGS, equation 3) also plays an important part in the formation of CO; (2) the equilibrium of the RWGS is highly sensitive to the outlet gas temperature from the electrolysis cell; and (3) the performance and syngas composition change significantly with the microstructure of SOECs and the operation conditions [11-13]. It also explains why tremendously different phenomena have been observed by different groups.

$$H_2O\,(g) \xrightarrow{electricity} H_2\,(g) + 1/2\,O_2\,(g) \qquad (1)$$

$$CO_2\,(g) \xrightarrow{electricity} CO\,(g) + 1/2\,O_2\,(g) \qquad (2)$$

$$CO_2\,(g) + H_2\,(g) \rightarrow CO\,(g) + H_2O\,(g) \qquad (3)$$

Up to now, the information available on HT steam/CO_2 coelectrolysis is very limited and previous studies primarily focus on novel materials development, performance characterization, and system efficiency analysis [14-18]. A number of fundamental questions still need to be answered. For example, the contribution of RWGS in the HT coelectrolysis process is still unclear. Carl M. Stoots [19] et al. report an area specific resistance (*ASR*) of 1.38 Ω cm^2 for HT coelectrolysis at 800°C, close to that 1.36 Ω cm^2 for HT steam electrolysis and much lower than that of 3.84 Ω cm^2 for HT CO_2 electrolysis, concluding that CO during HT steam/CO_2 coelectrolysis is primarily formed via the RWGS reaction. Nevertheless, M. Mogensen [1] and Zhongliang Zhan [20] et al. report similar *ASR* values with small difference for SOECs under the three different modes, inconsistent with the results of Carl M. Stoots et al.. Another issue regarding the relationship between the outlet syngas composition and the inlet gas composition, which can provide useful information on the control of the syngas composition, is still scarcely studied. Herein, a systematic study is conducted on HT steam/CO_2 coelectrolysis using the commercially available SOECs from Ningbo Institute of Industrial Technology to evaluate the performance, reaction characteristics, outlet gas composition and steam/CO_2 utilization of HT steam/CO_2 coelectrolysis under different operation conditions, including different inlet gas compositions and electrolysis current densities.

2. Experimental

All the button cells and single cells used in this study are purchased from Ningbo Institute of Industrial Technology. The SOECs are cathode-supported cells composed of Ni-YSZ (Y_2O_3-doped ZrO_2) cathode/YSZ electrolyte/ GDC (Gd_2O_3-doped CeO_2) buffer layer/ LSCF ($(La_{0.6}Sr_{0.4})(Co_{0.2}Fe_{0.8})O_3$) anode. The button cells are ~2.4 cm in diameter with an active area of 1cm^2 at the anode side. A single cell (10×10cm^2) with an active area of 64 cm^2 after the application of sealant is used during the study on the effect of the inlet gas composition on the performance and outlet gas compositions under a constant electrolysis current density of 0.15 A cm^{-2}. A single cell (5×5cm^2) with an active area of 16 cm^2 is used during the study on the influence of electrolysis current densities on the HT steam/CO_2 coelectrolysis between 0-1.0 A cm^{-2} considering the upper current limit of 22 A of the electrochemical workstation. The cross-section SEM image and photo of the single cell is shown in Fig.1.

A schematic of the apparatus used for HT steam/CO_2 coelectrolysis analysis is shown in Fig.2. The system is primarily composed of the corresponding gas bottles, mass flow controllers (MFC), a bubbler as the humidifier, humidity indicator (H), pressure gauges (P), thermometers (T), high temperature furnace, the solid oxide electrolysis cell, the dehumidifier to remove the steam in the outlet gas by cooling, the volumetric flow meter, and the Agilent 7820A gas chromatography (GC). H_2 is supplied to the single cell at a flow rate of 300 sccm for the reduction of the NiO particles in the cathode prior to the HT electrolysis measurements. In order to prevent the partial oxidation of the Ni particles in the

cathode, 20 mol. % of H_2 is used as the protection gas. In the anode, air is used as a sweeping gas at a flow rate of 300 sccm. CO_2 and H_2 at selected flow rate are controlled by the mass flow controller and directed into the humidifier to be mixed with the steam, whose content is changed and controlled by the water temperature in the humidifier. The accurate steam content is calculated and calibrated by the total pressure and humidity indicator placed at the exit of the humidifier via equation (4) below:

$$C_{s,i} = p_s H / P_t \quad (4)$$

where, $C_{s,i}$ is the steam content in the inlet gas, H is the relative humidity measured by the humidity indicator, p_s is the corresponding saturated steam pressure at the measured temperature and pressure, p_t is the total pressure measured by the pressure gauge. The flow rate of steam ($Q_{s,i}$) under the normal conditions is determined by equation (5):

$$Q_{s,i} = C_{s,i} (Q_{CO2,i} + Q_{H2,i}) / (1- C_{s,i}) \quad (5)$$

where, $Q_{CO2,i}$ and $Q_{H2,i}$ is the corresponding flow rate of CO_2 and H_2 controlled by the mass flow controller. During the button cell test, the total flow rate (Q_t) of the inlet gas is fixed at 100 sccm for the button cell test and 200 sccm for the single cell test. The temperature of the mixed gas from the humidifier is further elevated to ～150°C and a layer of heat insulating materials is applied outside the gas channel to avoid steam condensation, as indicated by the dashed line in Fig.2. The inlet gas is then directed into SOEC for HT coelectrolysis. The input and output

electrical signal is monitored by a Solatron 1260&1287 electrochemical workstation coupled with a 12V/20A power booster. The SOEC is heated and kept at a constant temperature of ~800°C by a furnace with integrated thermocouples. The outlet gas from the SOEC is directed into a dehumidifier, where the steam in the gas is removed. The volumetric flow rate (Q_O) and composition of the outlet gas is analysed by a volumetric flow meter and an Agilent 7820 gas chromatography. The utilization of steam (U_s) and CO_2 (U_{CO2}) is calculated according to equation (6-7) below:

$$U_s = (Q_O C_{H2,O} - Q_{H2,i}) / Q_{s,i} \quad (6)$$

$$U_{CO2} = Q_O C_{CO,O} / Q_{CO2,i} \quad (7)$$

where, $C_{H2,O}$ is the H_2 content in the outlet gas while $C_{CO,O}$ is the CO content in the outlet gas.

The impedance curves of the button cell at different atmospheres is measured with the Solatron 1260 impedance analyser in the frequency range from 100 kHz to 0.1 Hz with the amplitude of 10 mV at open circuit. The ohmic resistance (R_Ω) is measured from the high frequency intercept and the polarization resistance (R_p) is obtained from the differences between the high- and low-frequency intercepts on the impedance spectra. The *I-V* curve is measured in the voltage range of 0-0.6V at a scan rate of 50 mV s^{-1}.

3. Results and Discussion

One significant advantage of HT steam/CO_2 coelectrolysis lies in the

flexibility of adjusting the outlet syngas composition by varying the operation conditions, such as the inlet gas composition and the electrolysis current density [11, 17]. Therefore, the effect of the inlet gas composition on the electrochemical performance, outlet syngas composition, and the steam/CO_2 utilization is investigated. Fig.3 shows the electrochemical performance of HT steam/CO_2 electrolysis with different inlet gas compositions at 800°C using button cells. In the figure, the inlet gas with a CO_2 concentration of '0' corresponds to the atmosphere for HT steam electrolysis while the inlet gas with a CO_2 concentration of '80%' corresponds to the atmosphere for HT CO_2 electrolysis. In different atmospheres with variant steam/CO_2 concentration ratio, the cell maintains nearly constant (R_Ω) values with minor difference at 800°C, illustrating the stable electrode/electrolyte contact condition and ionic conductivity of the electrolyte [21]. The polarization resistance (R_p) is 0.32, 0.35, 0.31, 0.44 and 0.86 Ω cm^2 for the cell when the CO_2 content in the inlet gas is 0, 20%, 40%, 60% and 80%, respectively. It indicates that the inlet gas composition has significant influence on the related reaction kinetics only when the CO_2 content is above 60%. It is also supported by the area specific resistance (*ASR*) derived from the slope of the *I-V* curves in the electrolysis current density range of 0-0.6 A cm^{-2} (Fig.3b). *ASR* for the cell in different atmospheres is 0.75, 0.78, 0.70, 0.79 and 1.06 Ω cm^2 when the CO_2 content in the inlet gas is 0, 20%, 40%, 60% and 80%, respectively. The results confirm the superior performance of HT steam electrolysis and steam/CO_2 coelectrolysis to the HT CO_2 electrolysis, in agreement with the report of Carl. M.

Stoots [19] et al..

During the HT steam/CO_2 coelectrolysis process, two possible reactions, including the electrochemical reduction reaction of CO_2 (equation 2) and the RWGS chemical reaction (equation 3), may be responsible for the formation of CO. The *ASR* value, which has no direct relationship with the kinetics of the RWGS reaction, has a strong dependence on the performance of the electrochemical reduction of CO_2 and steam. As a result, it can be used to evaluate the contribution of the electrochemical reduction reaction in the formation of CO during HT steam/CO_2 coelectrolysis considering the much slower kinetics of HT CO_2 electrolysis over HT steam electrolysis. An increased *ASR* value should have been observed for HT steam/CO_2 coelectrolysis as the contribution of the electrochemical reduction reaction in CO formation increases. Nevertheless, similar *ASR* values for HT steam/CO_2 coelectrolysis and HT steam electrolysis are achieved here, proving that most the CO is formed via the RWGS reaction rather than the electrochemical reduction reaction. Considering the close Gibbs free energies (ΔG) for steam and CO_2 dissociation reaction at 800°C [9], the higher *ASR* values for HT CO_2 electrolysis may be caused by the poorer intrinsic catalytic activity of Ni-YSZ towards the electrochemical reduction reaction of CO_2 or the slower diffusion kinetics of the CO_2 over steam inside the porous electrode. The results of Zhongliang Zhan [20] et al. indicate that the calculated diffusion coefficient of steam at 800°C is $\sim$2.86 $cm^2\ s^{-1}$, two times that of 1.43 $cm^2\ s^{-1}$ for CO_2 at the same temperature, consistent with the observed increase in the

low-frequency arc in the nyquist plots, associated with the gas diffusion process, as the CO_2 concentration in the inlet gas of $H_2/H_2O/CO_2$ for HT steam/CO_2 coelectrolysis increases. So the slower diffusion kinetics of CO_2 over steam comprises one important reason for the increased *ASR* value while the CO_2 concentration in the inlet gas during HT steam/CO_2 coelectrolysis increases. Nevertheless, influence of the intrinsic catalytic activity of Ni-YSZ towards different electrochemical reactions can still not be excluded because it is still unclear whether Ni-YSZ has similar intrinsic catalytic activities towards the electrochemical reduction reactions of steam and CO_2 at the high temperature. A detailed investigation will be conducted in the future to clarify this question.

Fig.4 shows the open circuit voltage (*OCV*) of the single cell in different atmospheres at 800°C. Fig.5 shows the syngas composition and the steam/CO_2 utilization of the cell operated at 800°C under a constant current density of 0.15 A cm^{-2} after the removal of steam in the outlet gas. The single cell in pure hydrogen delivers a stable *OCV* value of ～1.10V during the test, indicating the good sealing effect. In the atmospheres for HT electrolysis, *OCV* is 0.89, 0.86, 0.88, 0.88 and 0.95 V when the CO_2 content in the inlet gas is 0, 20%, 40%, 60% and 80%, respectively. The slightly higher *OCV* value of 0.95V for HT CO_2 electrolysis at a CO_2 content of 80% is probably caused by the ～8% of CO formed via the RWGS reaction, as illustrated by the outlet syngas composition analysis in Fig.5a. The inlet gas composition does not have obvious influence on *OCV*, which can be explained in terms of the close Gibbs free energies for steam

and CO_2 splitting at 800°C [15].

At the open circuit condition, ～1-8% of CO is formed via the RWGS reaction in the atmospheres for HT coelectrolysis, depending on the CO_2 content in the inlet gas. The increase in the CO_2 content in the inlet gas results in the shift of the RWGS equilibrium to the right side and thereby the increased concentration of CO produced via the RWGS reaction. Compared with the CO and H_2 content at OCV, a significant increase in the CO and H_2 content is observed when an electrolysis current density of 0.15 A cm^{-2} is applied. For example, the H_2 content in the outlet gas increases from 15% at OCV to 30% at 0.15 A cm^{-2} while the CO content increases from 3% to 17% correspondingly at the inlet gas composition of 20% H_2 /40% steam /40% CO_2. It clearly demonstrates the effect of the input electric power on the outlet gas composition of the HT steam/CO_2 coelectrolysis system. However, a low steam/CO_2 utilization of ～20-40% is obtained due to the low electrolysis current density of 0.15 A cm^{-2} (Fig.5b). The H_2/CO content ratio in the outlet gas during HT steam/CO_2 coelectrolysis ranges from 6:1 to 1:1 with the inlet gas composition, confirming the feasibility of adjusting the syngas composition by controlling the inlet gas composition (Fig.5c). It should be noted that the 20% H_2 as the protection gas is also included in the outlet H_2 during the calculation process of the H_2/CO content ratio.

The outlet syngas composition and steam/CO_2 utilization are also measured at 800°C at different electrolysis current densities of 0-1.0 A cm^{-2} with a fixed inlet gas composition of 20% H_2 /40% steam /40% CO_2 and the corresponding results

are shown in Fig.6. In previous studies on HT steam/CO_2 coelectrolysis, a linear relationship in the whole current density range was observed in the plots of the CO, H_2 and CO_2 content in the outlet gas as a function of the current density [8, 19]. Two linear regions, including region I with a larger slope between 0-0.4 A cm^{-2} and region II with a lower slope between 0.4-1.0 A cm^{-2}, are clearly observed here, which may be ascribed to the different microstructure of the single cell and operation conditions adopted in the study. In region II, a slower increase in the H_2 and CO content appears as a function of the electrolysis current density, an obvious phenomenon of steam/CO_2 starvation at the cathode/electrolyte interface within the high current density region. It is also validated by the different *ASR* values calculated within the two regions. In region II, a much larger *ASR* of 1.35 Ω cm^2 is calculated compared to an *ASR* of 0.70 Ω cm^2 in region I (Fig.5d). Therefore, it is electrically more efficient to operate the HT coelectrolysis system at a current density below 0.4 A cm^{-2} within region I. Additionally, it is also relevant to expand the maximum current density in region I by optimizing the microstructure of SOECs to facilitate the diffusion process of the reactant gas.

Both of the H_2 and CO content in the outlet gas increases significantly with the electrolysis current density. A maximum value of 41% and 37% for H_2 and CO is observed at the current density of 1.0 A cm^{-2}. Meanwhile, the steam utilization increases from -8.0% at OCV to 76% at 1.0 A cm^{-2} and the CO_2 utilization increases from 13% to 77% accordingly. The negative steam utilization is attributed to the formation of CO through the RWGS reaction at the open circuit condition, which

consumes part of the 20% H_2 in the inlet gas as the protection gas of the Ni-YSZ composite cathode. Similarly, the H_2/CO content ratio also varies obviously with the current density from 1.9 at OCV, to 1.5 at 0.1 A cm^{-2}, 1.2 at 0.4 A cm^{-2} and 1.1 at 1.0 A cm^{-2}, indicating the high sensitivity of the outlet syngas composition to the electrolysis current density applied. During the synthesis of hydrocarbons or methanol from syngas via the catalytic processes, such as the Fisher-Tropsch process, the desired H_2/CO content ratio varies from ~1.4 to 2.1, which can be flexibly achieved by adjusting the operation conditions like the inlet gas composition or the electrolysis current density[22, 23]. It also comprises one important advantage of HT steam/CO_2 coelectrolysis. Therefore, the inlet gas composition and electrolysis current density are two important parameters which should be fully considered in the operation.

4. Conclusions

The reaction characteristics of syngas production by HT steam/CO_2 coelectrolysis with commercially available solid oxide electrolysis cells are systematically studied. During the inlet gas composition range (20% H_2 / 20-80% CO_2 / remaining steam) studied, the electrochemical performance of HT steam/CO_2 coelectrolysis is close to that of HT steam electrolysis and much superior to that of HT CO_2 electrolysis, supported by an *ASR* of 0.75 Ω cm^2 for HT steam electrolysis, 0.70-0.79 Ω cm^2 for HT coelectrolysis, and 1.06 Ω cm^2 for HT CO_2 electrolysis. It clearly indicates the important role of RWGS reaction in the formation of CO during the HT steam/CO_2 coelectrolysis process. The outlet syngas composition after the removal of steam varies significantly with a H_2/CO

content ratio of 1.0-6.0 as a function of the CO_2 concentration in the inlet gas and a ratio of 1.9-1.0 as a function of electrolysis current densities, confirming the feasibility of controlling the syngas composition by adjusting the operation conditions. The electrolysis current density has a significant influence on the steam/CO_2 utilization with a maximum value of 76% for CO_2 and 77% for steam at a high current density of 1.0 A cm^{-2}.

Acknowledgements

The project is supported by the Shell Global Solutions International B.V. and Shanghai CAS Advanced Research Institute under the Strategic Cooperation Agreement (Work Order No: PT31046).

References

1. S. D. Ebbesen, C. Graves and M. Mogensen, *International Journal of Green Energy*, 2009, **6**, 646-660.
2. S. D. Ebbesen, S. H. Jensen, A. Hauch and M. B. Mogensen, *Chemical Reviews*, 2014.
3. G. Hawkes, J. O'Brien, C. Stoots and B. Hawkes, *International Journal of Hydrogen Energy*, 2009, **34**, 4189-4197.
4. S. Li, Y. Li, Y. Gan, K. Xie and G. Meng, *Journal of Power Sources*, 2012, **218**, 244-249.
5. Q. Fu, C. Mabilat, M. Zahid, A. Brisse and L. Gautier, *Energy & Environmental Science*, 2010, **3**, 1382-1397.
6. S.-E. Yoon, S.-H. Song, J. Choi, J.-Y. Ahn, B.-K. Kim and J.-S. Park, *International Journal of Hydrogen Energy*, 2014, **39**, 5497-5504.
7. W. L. Becker, R. J. Braun, M. Penev and M. Melaina, *Energy*.
8. Q. Fu, J. Dailly, A. Brisse and M. Zahid, *ECS Transactions*, 2011, **35**, 2949-2956.
9. C. Graves, S. D. Ebbesen, M. Mogensen and K. S. Lackner, *Renewable and Sustainable Energy Reviews*, 2011, **15**, 1-23.
10. J. E. O'Brien, M. G. McKellar, E. A. Harvego and C. M. Stoots, *International Journal of Hydrogen Energy*, 2010, **35**, 4808-4819.
11. C. M. Stoots, *HIGH-TEMPERATURE CO-ELECTROLYSIS OF H2O AND CO2 FOR SYNGAS PRODUCTION*, 2006.

12. V. Menon, Q. Fu, V. M. Janardhanan and O. Deutschmann, *Journal of Power Sources*, 2015, **274**, 768-781.
13. Y. Xie and X. Xue, *Solid State Ionics*, 2012, **224**, 64-73.
14. K. Xie, Y. Zhang, G. Meng and J. T. S. Irvine, *Energy & Environmental Science*, 2011, **4**, 2218-2222.
15. X. Sun, M. Chen, S. H. Jensen, S. D. Ebbesen, C. Graves and M. Mogensen, *International Journal of Hydrogen Energy*, 2012, **37**, 17101-17110.
16. C. Graves, S. D. Ebbesen and M. Mogensen, *Solid State Ionics*, 2011, **192**, 398-403.
17. M. Ni, *Journal of Power Sources*, 2012, **202**, 209-216.
18. P. Kim-Lohsoontorn and J. Bae, *Journal of Power Sources*, 2011, **196**, 7161-7168.
19. C. Stoots, J. O'Brien and J. Hartvigsen, *International Journal of Hydrogen Energy*, 2009, **34**, 4208-4215.
20. Z. Zhan, W. Kobsiriphat, J. R. Wilson, M. Pillai, I. Kim and S. A. Barnett, *Energy & Fuels*, 2009, **23**, 3089-3096.
21. X. Chen, C. Jin, L. Zhao, L. Zhang, C. Guan, L. Wang, Y.-F. Song, C.-C. Wang, J.-Q. Wang and S. P. Jiang, *International Journal of Hydrogen Energy*, 2014, **39**, 15728-15734.
22. G. A. Mills, *Fuel*, 1994, **73**, 1243-1279.
23. E. Iglesia, *Applied Catalysis A: General*, 1997, **161**, 59-78.

List of figures

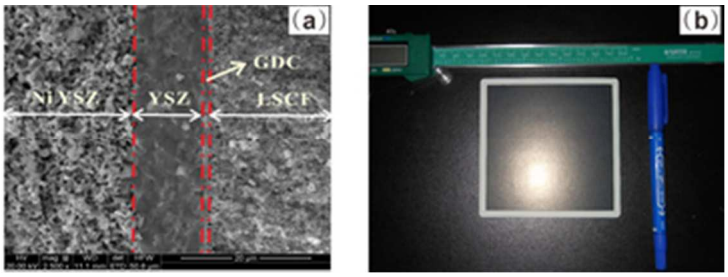

single column (8.3cm)
30x11mm (300 x 300 DPI)

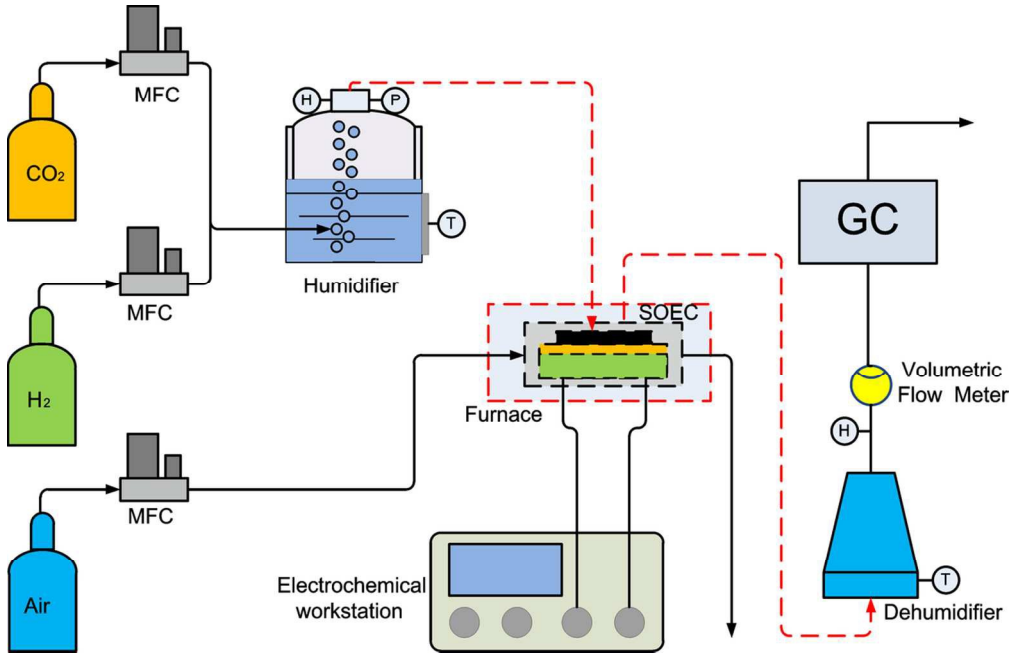

Double column (17.1cm)
110x71mm (300 x 300 DPI)

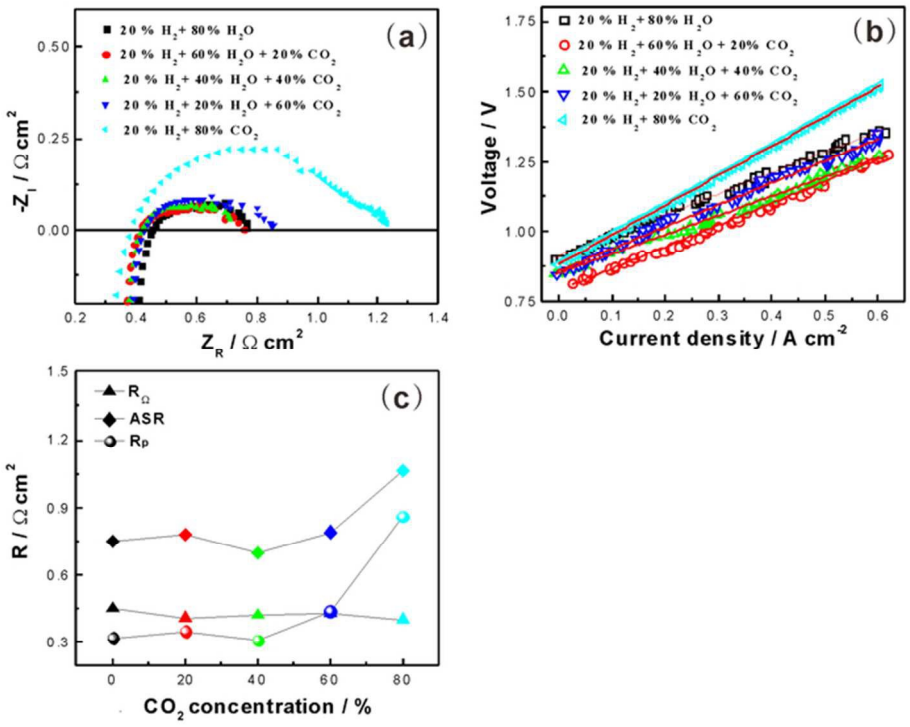

single column (8.3cm)
64x50mm (300 x 300 DPI)

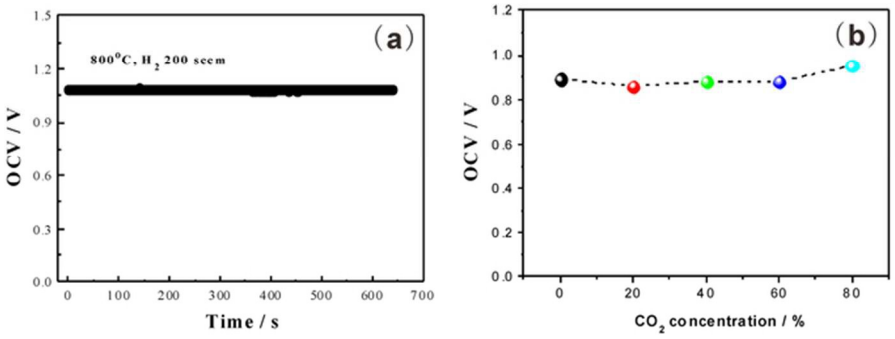

single column (8.3cm)
64x24mm (300 x 300 DPI)

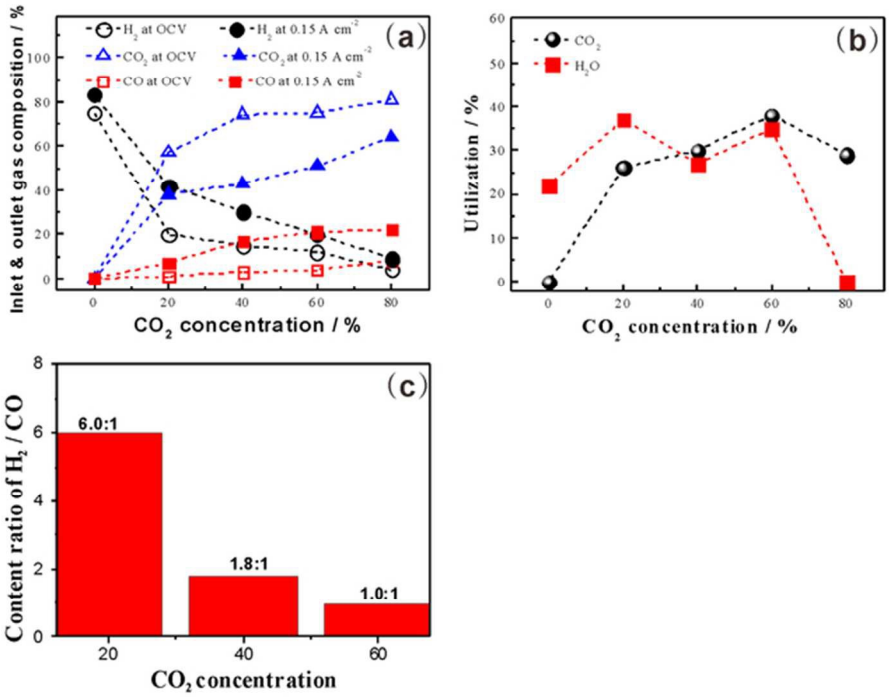

single column (8.3cm)
60x44mm (300 x 300 DPI)

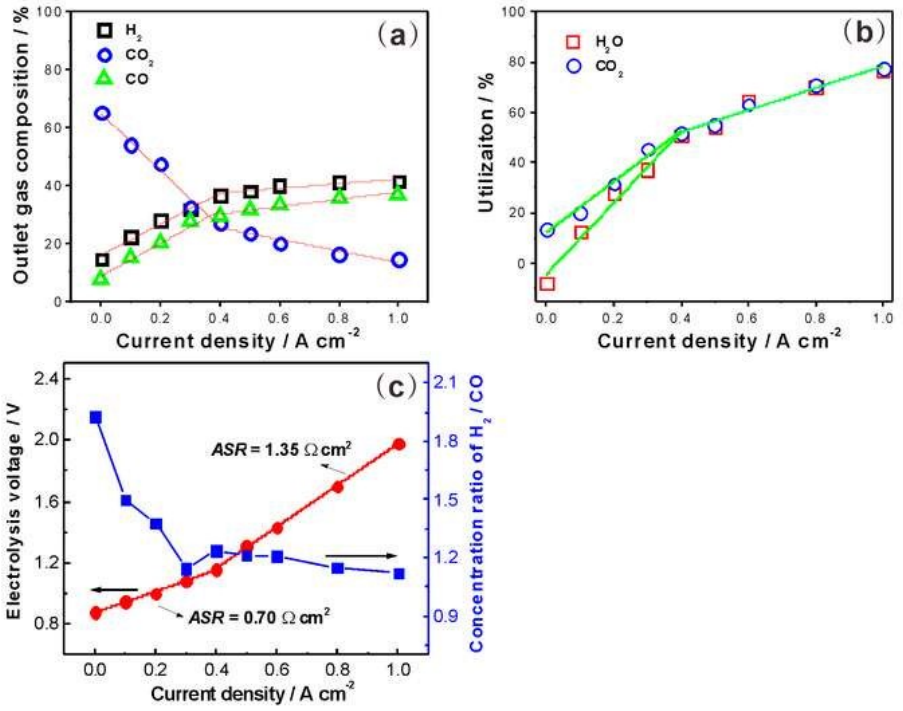

single column (8.3cm)
63x47mm (300 x 300 DPI)